

# Evaluation of Eye-Blinking Dynamics in Human Emotion Recognition Using Weighted Visibility Graph

Atefeh Goshvarpour<sup>1</sup>, Ateke Goshvarpour<sup>2,3\*</sup> 

<sup>1</sup> Department of Biomedical Engineering, Faculty of Electrical Engineering, Sahand University of Technology, Tabriz, Iran

<sup>2</sup> Department of Biomedical Engineering, Imam Reza International University, Mashhad, Razavi Khorasan, Iran

<sup>3</sup> Health Technology Research Center, Imam Reza International University, Mashhad, Razavi Khorasan, Iran

\*Corresponding Author: Ateke Goshvarpour  
Email: [ak\\_goshvarpour@imamreza.ac.ir](mailto:ak_goshvarpour@imamreza.ac.ir)

Received: 14 October 2022 / Accepted: 15 December 2022

## Abstract

**Purpose:** Designing an automated emotion recognition system using biosignals has become a hot and challenging issue in many fields, including human-computer interferences, robotics, and affective computing. Several algorithms have been proposed to characterize the internal and external behaviors of the subjects in confronting emotional events/stimuli. Eye movements, as an external behavior, are habitually analyzed in a multi-modality system using classic statistical measures, and the evaluation of its dynamics has been neglected so far.

**Materials and Methods:** This experiment intended to provide an innovative single-modality scheme for emotion classification using eye-blinking data. The dynamics of eye-blinking data have been characterized by weighted visibility graph-based indices. The extracted measures were then fed to the different classifiers, including support vector machine, decision tree, k-Nearest neighbor, Adaptive Boosting, and random subset to complete the process of classifying sad, happy, neutral, and fearful affective states. The scheme has been evaluated utilizing the available signals in the SEED-IV database.

**Results:** The proposed framework provided significant performance in terms of recognition rates. The highest average recognition rates of  $> 90\%$  were achieved using the decision tree.

**Conclusion:** In brief, our results showed that eye-blinking data has the potential for emotion recognition. The present system can be extended for designing future affect recognition systems.

**Keywords:** Dynamics; Emotion Recognition; Eye-Blinking; Weighted Visibility Graph.

## 1. Introduction

Emotion is a subjectively experienced complex reaction that usually affects a human's response and behavior toward a specific object. In addition, emotion is typically along by physiological and behavioral fluctuations in the body [1, 2]. The importance of assessing emotions in human behavior and life has attracted researchers to provide a highly accurate emotion recognition system by examining various signal processing and machine learning frameworks. Currently, these systems receive diverse applications, like Human-Computer Interfaces (HCI) and robotics [3].

Up to now, a broad range of signals has been recruited to design an affect recognition system. The systems have been applied in a multi/single-modality or multi/single-channel form. Multi-channel/modality systems can recognize emotions since they combine information from multiple sources. On the contrary, a single-channel/modality is preferable to a multi-channel/modality structure in terms of computing costs, time-consuming, and speed of calculation. Additionally, they are rarely involved in the daily activities of the subject. The most commonly used signals are the ElectroEncephaloGram (EEG), Heart Rate Variability (HRV), ElectroCardioGram (ECG), Galvanic Skin Responses (GSR), PhotoPlethysmoGraphy (PPG), and facial ElectroMyoGrams (EMG) [4-16]. All of these signals convey the internal behaviors of a participant in confronting affective stimuli. External behaviors, like eye movements, also have the potential to provide information about the person's emotions [17, 18].

Eye activity is monitored routinely by image or video frame processing. Preparing these images requires the observance of restrictive pre-determined/controlled laboratory conditions. The face should be toward a standard camera, and any movement of the head, reorientation of the camera, face mask, or eyeglasses can restrict these systems [19]. One way to overcome these problems is to use a signal processing-based system that analyzes ElectroOculoGram (EOG) to estimate ocular activity. Most studies on emotion recognition have utilized the image-processing approach to access visual information. For example, the work performed by Al-gawwam and Benaissa [20] analyzed the blinking of depressed and non-depressed people by processing video frames obtained from the face. In this study, we

intended to use blink information obtained from EOG analysis.

Most previous emotional studies have used a multimodal approach, which combines eye activities with other signals. For positive, neutral, and negative emotion classification, Lu *et al.* [17] proposed a system through EEG and eye movement data. The team testified that manipulating a multimodal structure increases the accuracy of the recognition rates, where the best accuracy was 87.59%. In contrast, the highest accuracy rates of 77.8% and 78.51% were reported using eye movements and EEG, respectively. Zheng *et al.* [18] attempted to classify four emotions of happiness, sadness, fear, and neutral by merging a six-electrode EEG and eye movement data. They achieved the best mean accuracy of 85.11% using deep neural networks. Some researchers have also analyzed eye movement patterns in patients with emotional deficits, like Parkinson's disease [21, 22], depression [20], conduct disorder [23], autism [24], and hypomanic personality traits [25].

To the best of our knowledge, eye movements, in a single-modality form, have been used in limited experiments for the emotion recognition of healthy participants [26, 27]. Alghowinem *et al.* [26] inspected the potential of eye activity in the manifestations of emotional states using an eye-tracking sensor. The authors recorded the eye activities of 60 female participants during the exposure to positive and negative emotions. Then, some statistical and low-level features were extracted and fed into the Support Vector Machine (SVM) for emotion recognition. The proposed scheme achieved a maximum accuracy of 66%. Subsequently, the authors acclaimed the potential of eye movements, pupil enlargement, or invisibility to the eye tracker as a complementary cue for emotion detection [26]. Tarnowski *et al.* [27] proposed an eye-tracking emotion recognition system. They extracted pupil diameter, the fixations, and the saccades' eye movements and fed them to the SVM. They reported the highest accuracy of 80%. Currently, we explored the competency of eye-blinking data as an indication of emotional states. For the first time, we intended to evaluate the eye-blinking information in an emotion recognition problem using a weighted visibility graph.

Typically, biosignal analysis relies on different features, including conventional time-domain and frequency-domain indices and nonlinear measures. Biomedical signals have chaotic and non-stationary nature

[28]. This property makes the standard approaches insufficient to characterize these signals. Therefore, there is unceasing research towards the expansion of innovative methods that can detect relevantly important information about biosignals concerning their nonlinear dynamics behavior [13, 14]. Recently, a nonlinear signal analysis approach that leads to the formation of complex networks has become an active area of research. The concept of a complex network for projecting a time series was proposed by Zhang *et al.* [29]. This projection could provide further information about hidden signal patterns by utilizing different network characteristics, like statistical measures. Two years later, a visibility graph was presented to convert a time series into a map in the light of the complex network theory [30]. This method is straightforward with a fast computational algorithm and can quantify the nonlinear characteristics of the time series. The visibility graph method has the advantage that it does not require pre-processing and noise removal compared to conventional methods [31]. By applying any of them, part of the signal information is lost. These reasons motivate us to use a visibility graph technique characterizing eye-blinking signals in emotion recognition.

Different biomarkers have been extracted from this analytical method that can effectively identify various pathological and psychological conditions [32-36]. In addition, the visibility graph has been utilized effectively to analyze and interpret some biosignals. Zhu *et al.* [37] classified the sleep stages using graph-based indices from a single-channel EEG. Using an SVM, they examined the potency of the features in discriminating the sleep stages into two to six phases. An accuracy of 87.5% was reported for the six-state classification. Supriya *et al.* [34] converted the EEG time series into a weighted visibility graph to detect epileptic seizure activity. SVM and k-Nearest Neighbor (kNN) obtained the performances of 100% for discrimination between the ictal and healthy normal. In another study [38], an improved visibility graph algorithm, namely the limited penetrable visibility graph, was proposed to examine the EEG dynamics of patients with Alzheimer's disease. A grouped horizontal visibility entropy was proposed for analyzing the interbeat intervals [39]. The superiority of the suggested technique for characterizing the dynamics of humans' activity levels was reported. Bhaduri *et al.* [40] proposed a chaos-based modified visibility graph framework. They recruited the approach to analyze the dynamics of the speech signals for the assessment of a precursor of the suicidal tendency. Samanta *et al.* [41] proposed a framework employing a

multiplex weighted visibility graph in combination with the Random Forest classifier for classifying motor imagery EEG signals. They achieved an average classification accuracy of ~ 99.9%. As the review of the articles shows, most of the analyses have been done on EEG signals. On the other hand, a visibility graph-based method for recognizing emotions has not been utilized.

We intended to find whether eye movement, as a separate modality, can be used to recognize emotional classes with appropriate accuracy. In addition, are the signal dynamics obtained by the visibility graph capable of separating emotion groups? In this study, we aimed to develop a single-modality emotion recognition system using eye-movement data. We analyzed the eye-blinking signals of 15 participants while watching emotive video clips. The videos were intended to evoke four happy, sad, fearful, and neutral emotions. First, the weighted visibility graph of the signals was reconstructed. To characterize each map, we extracted two innovative indices based on the weights of the edges and the shortest path length between any two vertices of the network. Next, the features were fed to the SVM. The proposed human emotion recognition scheme is shown in Figure 1.

## 2. Materials and Methods

### 2.1. Data

In this experiment, we analyzed the freely available eye movement data in the SEED-IV database [18]. The database includes 15 healthy right-handed subjects. The recordings belong to eight females and seven males in the age range of 20 and 24 years. Each individual participated in three different test sessions on definite days to maintain protocol stability after a while. Consequently, the recordings of three sessions for each participant and a total of 45 data were obtained.

To provoke emotions, 72 film clips were presented. The videos contained four target excitements, including sad, fearful, happy, and neutral. The duration of each clip was about two minutes, offered exclusively once to avoid duplication. In each session, six trials per emotion were presented. Each test comprised a 5-second hint for starting, a clip presentation for about two minutes, and a 45-second self-assessment. A self-assessment was performed after each clip using the PANAS scales. Rather

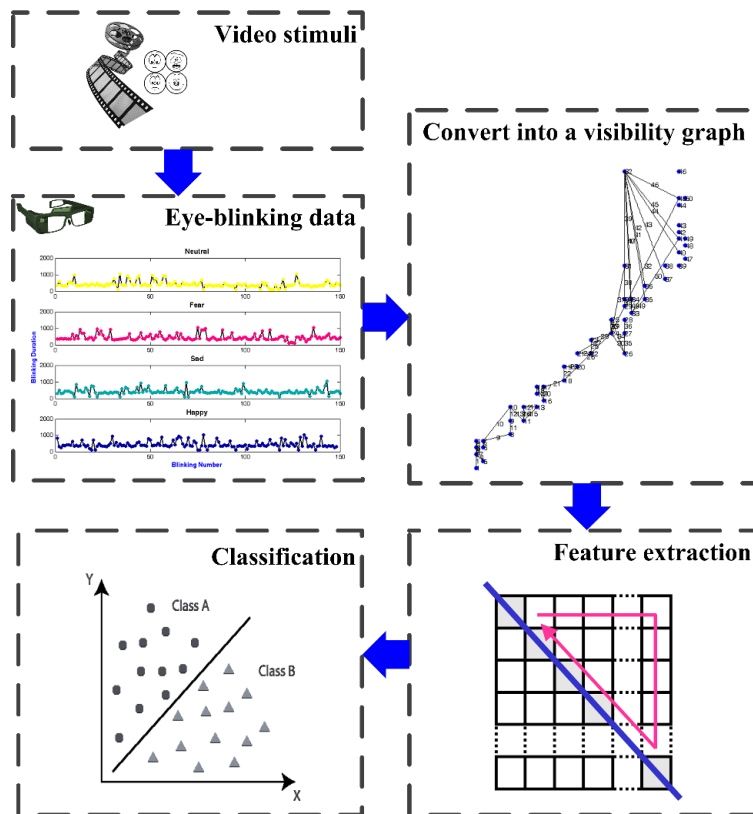


**Figure 1.** The proposed scheme. First, the participants' eye-blinking signals were taken from [18] while watching emotional video clips. Next, these time series were converted into visibility graphs. By analyzing the graphs, two features were extracted to quantify the dynamical properties of the signal. Finally, the characteristics were applied to the classification module to recognize emotions

than what the participants thought the emotion should be, the films were rated based on how they felt in reality while watching. Data were excluded when the subject could not evoke real or strong enough arousal emotions [18]. Figure 2 schematically illustrates the protocol of emotion experiments.

Wearable eye-tracking glasses, SensoMotoric Instruments Eye Tracking Glasses (SMI ETG), were used to record eye movements. For further steps, we

analyzed the eye-blinking data from all participants in all sessions. Figure 3 exhibits an instance of the data in various emotions. The figure shows that the blink duration was different in the clips with different emotions. For example, happy clip duration has a higher range than other emotions. Previous literature [42] highlighted that blink rate is an attention index during emotional clip viewing. The highest blink rate inhibition, showing greater attention to the stimuli, was concluded during the

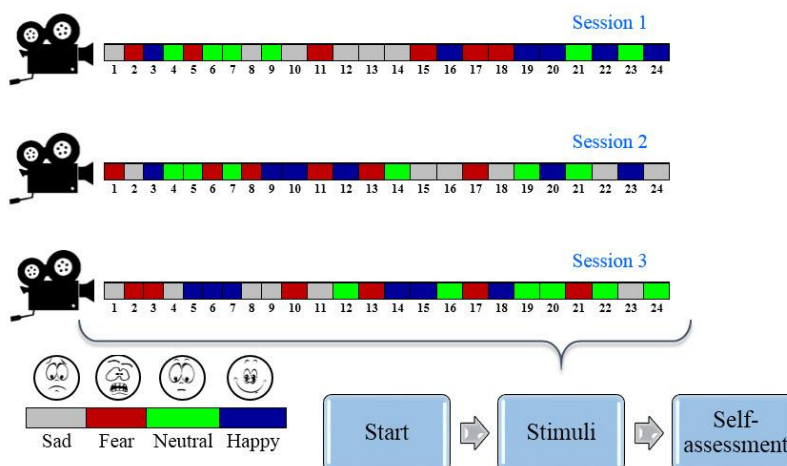


**Figure 2.** The emotion elicitation protocol

presentation of erotic, scenery, and compassion clips. On the contrary, the smallest blink rate inhibition was obtained for fear clips, which derived a defensive reaction with motivation rejection. Blink rate across time confirmed that compassion (sadness) stimuli evoked early (a slower, later) inhibition.

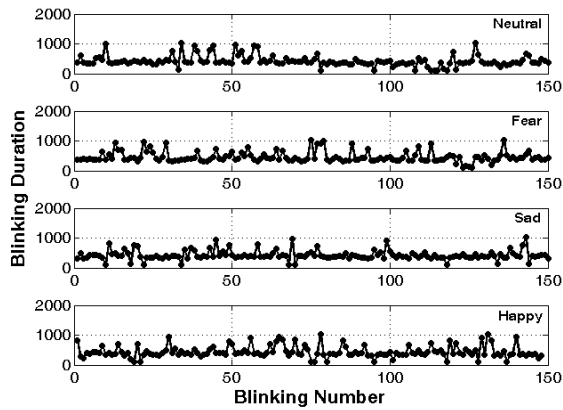


**Figure 3.** An illustration of eye-blinking data in four emotional states (subject 12, session 2). The blink duration is in milliseconds (ms), shown on the vertical axis. The horizontal axis shows the blinking number. It is noted that in each session, signals related to a similar emotion were put together, and 150 samples of them were shown in the figure

## 2.2. Feature Extraction

### 2.2.1. Weighted Visibility Graph

To transform data into a weighted visibility graph, firstly, the nodes of the graph should be defined. Consider the eye-blinking time series as a scalar measure  $x_i (i = 1, 2, \dots, N)$  with  $N$  sample points. A weighted visibility graph of the data ( $VG(N, E)$ ) involves  $N = \{n_i\} (i = 1, 2, \dots, N)$  as nodes and  $E = \{e_i\} (i = 1, 2, \dots, N)$  as edges. Each data sample reflected a graph node.

This study implemented the natural VG algorithm to define the links between different nodes of the VG [30]. According to the Euclidean plane, for the VG reconstruction, each node characterizes the position of a point, and links between relevant vertices have exclusively existed if they are visible to each other. To evaluate whether the edges between any two pairs of nodes exist, the following decree should be fulfilled, called a partial convexity constraint (Equation 1):

$$X_z < X_x + (X_y - X_x) \frac{z - x}{y - x}, \quad x < z < y \quad (1)$$

Where  $x$  and  $y$  are two random time events and  $z$  is the time event between them,  $X_x = X(x)$ ,  $X_y = X(y)$ , and  $X_z = X(z)$  are the data sample points. Figure 4 shows an example of a time series with its corresponding VG.

To define a Weighted Graph (WVG), the edge weights between two nodes should be determined. We defined the edge weight according to the following Equation 2:

$$W_{xy} = \arctan \frac{X_y - X_x}{y - x}, \quad x < y \quad (2)$$

Where  $W_{xy}$  is the edge weight between node  $n_x$  and node  $n_y$ , and the weights are in a radian. The arctan refers to an inverse trigonometric function. This function is implemented to identify the sudden variation in the signals. To clarify the benefit of the weight, suppose a time-series  $X = \{87, 49, 36, 49, 83, 47\}$  with time  $t = \{1, 2, 3, 4, 5, 6\}$  (Figure 4).

Figure 4 revealed that for  $x = 2$  and  $y = 4$ ,  $X_x = X_y = 49$ . Therefore, both are having the same value. On the other hand, a sudden variation has occurred at  $z = 5$ , where  $X_z = 83$ . Using Equation 2, the edge weight between  $X_x$  and  $X_z$  and the edge weight between  $X_y$  and  $X_z$  are calculated as follows (Equations 3, 4):

$$W_{xz} = \arctan \frac{X_z - X_x}{z - x} = \arctan \frac{83 - 49}{5 - 2} = 1.4828 \quad (3)$$

$$W_{yz} = \arctan \frac{X_z - X_y}{z - y} = \arctan \frac{83 - 49}{5 - 4} = 1.5414 \quad (4)$$

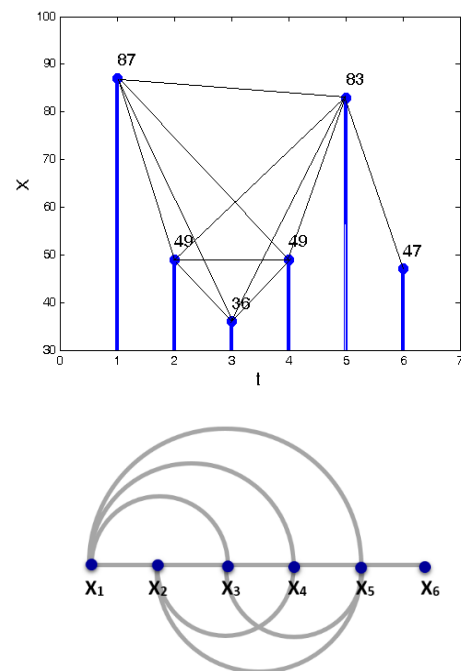


**Figure 4.** An example of a visibility graph for data. (a) A time-series data, (b) corresponding visibility graph

Therefore, even if two data samples have the same values, their binding strength to the third node will vary according to their edge weight.

### 2.2.2. WVG Characterization

To characterize WVG, we have defined two measures (F1 and F2). These measures were calculated as follows:

F1: The total weights of all the edges were considered as Equation 5:

$$W_T = \left| \sum_{i,j} W_{ij} \right| \tag{5}$$

where i and j represent different nodes of the graph.

F2: We first find the distances between any vertices of the graph, which achieved a square matrix ( $M_D$ ). The shortest path length between any two vertices of the network is considered the distance between them. The distances were calculated using the Graph Theory toolbox for MATLAB [43], which benefits from the Floyd-Warshall algorithm [44]. Then, we sum up all the elements of the upper triangular part of  $M_D$ . Figure 5 and Equation 6 show schematically how this feature is estimated from the  $M_D$ .

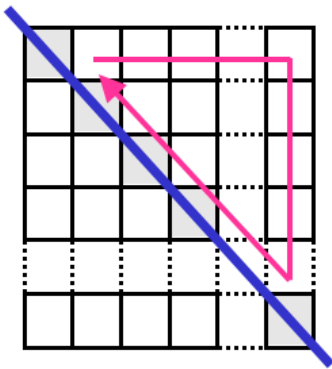


Figure 5. An illustration of F2 calculation from MD

$$\begin{aligned}
 M_{D(n \times n)} &= \begin{bmatrix} 0 & D_{12} & D_{13} & \dots & D_{1n} \\ D_{21} & 0 & D_{23} & \dots & D_{2n} \\ D_{31} & D_{32} & 0 & \dots & D_{3n} \\ \vdots & \vdots & \vdots & \ddots & \vdots \\ D_{n1} & D_{n2} & D_{n3} & \dots & 0 \end{bmatrix} \rightarrow TUM_D \\
 &= \begin{bmatrix} D_{12} \\ D_{13} \\ D_{23} \\ \vdots \\ D_{1n} \\ D_{2n} \\ D_{3n} \\ \vdots \\ D_{(n-1)n} \end{bmatrix} \rightarrow F2 \\
 &= \left| \sum_{i=1}^{(n-1)n} TUM_D(i) \right|
 \end{aligned} \tag{6}$$

Where  $D_{xy}$  is the distance between vertex x and vertex y of the graph, and  $TUM_D$  represents the upper triangular matrix of the  $M_D$ .

The  $M_D$  is a symmetric matrix ( $D_{xy} = D_{yx}$ ). The diagonal elements of the  $M_D$  are zero. Therefore, the complete  $M_D$  measures can be shown by strictly upper/lower triangular matrix elements

## 2.3. Classification

### 2.3.1. Support Vector Machine

SVM transformed the input features into a high-dimensional space. Compared to the original input features, a transformed one contributes a more trivial task to separate data. Contingent upon the input, an iterative learning operation provides an optimum hyperplane with the maximum margin between the groups in a high-dimensional feature space. Lastly, the maximum-margin hyper-planes will outline the decision borders over the data clusters [45]. The higher distance between hyper-planes and data points in miscellaneous categories the higher classification rates. SVM drives with the taking on a kernel function, which befalls a nonlinear one. The current study employed a Radial Basis Function (RBF) as a kernel function. A sub-sampling procedure has been used to select the scale value of the kernel.

### 2.3.2. k-Nearest Neighbor (kNN)

kNN is a non-parametric and supervised classifier. It incorporates a well-defined distance calculation. In this approach, the new sample query outcome is categorized relying upon the contiguity of the k-nearest examples easily gotten in the feature space [46,47]. In this experiment, we evaluated different k values (k), where k represents the number of neighbors in the classification model, to calculate the classification outcomes. Precisely, we have reported the performance of the 2NN, 3NN, 4NN, 5NN, 6NN, 7NN, 8NN, 9NN, and 10NN.

### 2.3.3. Decision Tree (DT)

DT is a decision tool. It indicates the possible result of a decision such as the consequence of the event, groups or group distributions, and the resource outflows using a tree-like model [46]. It adopts a set of hierarchical decisions on the features for classification.

### 2.3.4. Adaptive Boosting and Random Subspace

Ensemble methods belong to machine learning algorithms. For these methods, multiple “weak learners” are used to solve the same problem and fused to catch better outcomes compared to any of the constituent learning procedures alone. Bagging and boosting are two main subgroups of ensemble methods.

Bagging is a shortened form of “bootstrap aggregating”. It involves a separate model in the ensemble vote with one and identical weight. To uphold model variance, this method trains each learning procedure in the ensemble using an arbitrary subset of the training set. Boosting implicates incrementally constructing an ensemble through training each new instance to accentuate the training cases that former learning procedures misclassification. Adaptive Boosting (AdaBoost) is the most common boosting procedure. The “random subspace; RS” learning procedure is comparable to bagging, excluding that the features are randomly sampled with a replacement for each learner.

Before involving the measures in the classifier, the indices were normalized as follows (Equation 7):

$$\text{Normalized } F = 2 \left( \frac{F - F_{\min}}{F_{\max} - F_{\min}} - 1 \right) \quad (7)$$

Where  $F$  denotes the feature set. The feature set is a matrix, in which the samples were included in the rows, and the features, F1, and F2 formed the columns.

Here, a One Vs. All (OVA) classification strategy was adopted. The classification was performed by a 10-fold cross-validation scheme, which brings about the benefits of avoiding over-fitting. Accuracy (Ac), sensitivity (Se), and specificity (Sp) were calculated to evaluate the performance of the classifier. In addition, the Receiver Operating Characteristic (ROC) curve was reconstructed, and the Area Under the Curve (AUC) was calculated. All simulations were performed using MATLAB software on a VAIO laptop series SR.

## 3. Results

The WVG of the time series in different emotional states was reconstructed and two measures, F1 and F2, were calculated. Figure 6 shows the box plot diagram of the features.

As the figure shows, a higher total weight of edges was achieved for fear (Figure 6a). A greater F2 value

was obtained during sadness stimuli (Figure 6b). The lowest F1 value was obtained for the happy state (Figure 6a). In contrast, the lowest value of F2 was obtained for neutral (Figure 6b).

For a 50-time run of the classification procedure, the mean and standard deviation of the accuracy have been provided in Table 1. In addition, the maximum Ac, and the corresponding Se, Sp, and AUC have been listed in Table 1.

The results of Table 1 indicated that DT outperformed the other classifiers. DT reached the maximum accuracy of 100% for the classification of fear, neutral, and happy states. The corresponding sensitivity and specificity were 100%. The average accuracy of DT for recognition of these states was also > 90%. The second-best classification results were achieved using RS, where the maximum accuracy was > 88% for emotion recognition. In contrast, the lowest rates were obtained using kNN and SVM. For different kNN structures, the highest average accuracy was 76%. The highest average accuracy was 77% using SVM. The AUC of all classifiers was above 0.7.

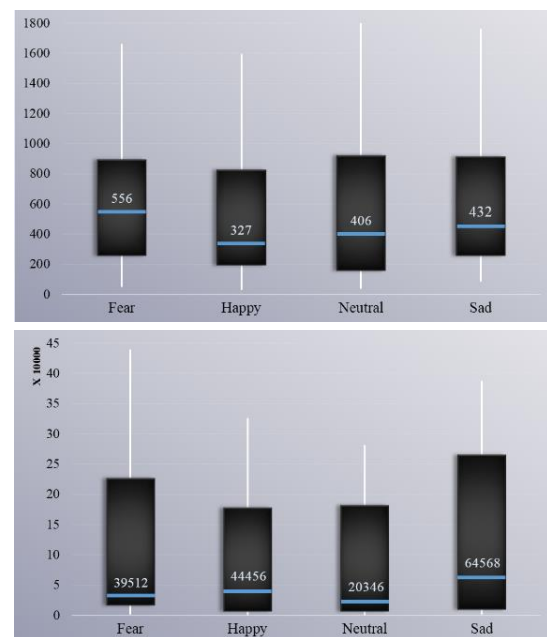


**Figure 6.** The variability of the WVG measures in different emotional states, including fear, happiness, neutral, and sad; (a) F1, (b) F2. The average values have been specified by blue lines. Additionally, their numerals have been printed on each box.

The bottom side of the filled box is the first quartile, which separates 25% of the data from the rest and the top side of the filled box shows the third quartile. The endpoint of the white lines from the box at the bottom and the top are the minimum and maximum values in the feature. The distance between the endpoints is termed the range

**Table 1.** The human emotion recognition rates using eye-blinking data in a 10-fold cross-validation scheme

Classifier	Class	k for kNN	Ac (mean ± SD)	Ac (Max.)	Se	Sp	AUC
SVM	<i>F vs. all</i>	-	74 ± 3.78	88.89	100	87.50	1.00
	<i>S vs. all</i>	-	71.22 ± 3.53	83.33	95.83	82.89	0.97
	<i>N vs. all</i>	-	77.33 ± 3.8	88.89	75.00	92.86	0.84
	<i>H vs. all</i>	-	74.33 ± 3.84	88.89	100	87.50	1.00
DT	<i>F vs. all</i>	-	<b>91.89 ± 2.26</b>	<b>100</b>	100	100	1.00
	<i>S vs. all</i>	-	85.89 ± 2.12	94.44	100	95.40	1.00
	<i>N vs. all</i>	-	<b>90.56 ± 1.88</b>	<b>100</b>	100	100	0.96
	<i>H vs. all</i>	-	<b>91 ± 2.24</b>	<b>100</b>	100	100	1.00
AdaBoost	<i>F vs. all</i>	-	79.56 ± 1.42	88.89	100	87.5	1.00
	<i>S vs. all</i>	-	80 ± 1.37	83.33	100	82.73	1.00
	<i>N vs. all</i>	-	86.87 ± 2.23	94.44	94.29	96.05	0.96
	<i>H vs. all</i>	-	<b>90.33 ± 1.85</b>	94.44	100	94.96	1.00
RS	<i>F vs. all</i>	-	78.33 ± 3.07	88.89	90	90.6	0.93
	<i>S vs. all</i>	-	76.78 ± 2.67	88.89	82.22	93.27	0.89
	<i>N vs. all</i>	-	81.89 ± 3.26	94.44	100	100	1.00
	<i>H vs. all</i>	-	77.45 ± 3.52	94.44	100	93.33	1.00
<i>F vs. all</i>		2	48.89 ± 11.45	77.78	50	81.25	0.71
		3	69.44 ± 6.47	83.33	100	82.35	1.00
		4	64.44 ± 10.65	94.44	100	93.33	1.00
		5	71.22 ± 6.61	77.78	50	81.25	0.71
		6	68.11 ± 9.24	83.33	66.67	86.67	0.8
		7	71.89 ± 7.05	83.33	100	82.35	1.00
		8	71.45 ± 7.1	83.33	100	82.35	1.00
		9	76 ± 3.8	83.33	100	82.35	1.00
		10	73.45 ± 5.64	83.33	100	82.35	1.00
	<i>S vs. all</i>		2	60 ± 10.74	83.33	60	92.31
		3	73.89 ± 8.41	88.89	75	92.86	0.84
		4	64.78 ± 10.39	83.33	66.67	86.67	0.8
		5	70.11 ± 8.34	83.33	100	82.35	1.00
		6	68.56 ± 8.22	88.89	75	92.86	0.84
		7	71.44 ± 7.01	83.33	100	82.35	1.00
		8	71.56 ± 8.22	83.33	100	82.35	1.00
		9	73.22 ± 6.01	83.33	100	82.35	1.00
		10	73.67 ± 6.81	88.89	75	92.86	0.84
kNN		<i>N vs. all</i>	2	60 ± 11.52	77.78	57.14	100
	3		70 ± 8.25	77.78	100	87.5	1.00
	4		64.22 ± 10.83	88.89	75	92.86	0.84
	5		75.56 ± 6.91	83.33	100	82.35	1.00
	6		64.78 ± 9.22	83.33	66.67	86.67	0.8
	<i>H vs. all</i>	7	70.89 ± 5.99	77.78	100	82.35	1.00
		8	69.22 ± 6.85	77.78	66.67	86.67	0.8
		9	75.22 ± 4.23	83.33	100	82.35	1.00
		10	71.67 ± 6.5	83.33	100	82.35	1.00
		2	56.22 ± 10.44	77.78	50	100	0.61
<i>H vs. all</i>	3	65.67 ± .96	83.33	100	82.35	1.00	
	4	65.22 ± 8.38	77.78	50	85.717	0.68	
	5	69.44 ± 7.21	83.33	100	82.36	1.00	
	6	65.22 ± 9.51	83.33	66.67	86.67	0.8	
	7	73.89 ± 6.27	88.89	100	87.5	1.00	
	8	72.56 ± 5.43	88.89	100	87.5	1.00	
	9	75 ± 3.59	83.33	100	82.35	1.00	
	10	73 ± 5.83	83.33	100	82.35	1.00	

Note –N: Neutral, F: Fear, S: Sad, and H: Happy. Ac: Accuracy, Se: Sensitivity, Sp: Specificity, AUC: Area under ROC curve

## 4. Discussion

Developing computerized human emotion recognition systems becomes a challenging issue in human-computer interaction. A typical system aimed to automatically identify, respond to, and manage users' emotions while facilitating communication between humans and machines. However, recognizing human emotions has been associated with several challenges, including ease of use and user-friendliness, which were not obtainable by previous multimodal schemes. In this experiment, an innovative methodology for human emotion recognition was presented using eye-blinking data. We analyzed publicly available eye-blinking data from the SEED-IV database [18]. The weighted visibility graph of the signals was reconstructed to develop a computerized human emotion recognition system. Next, we proposed two novel measures of the graph.

Ultimately, different classifiers were employed to discriminate emotions using a 10-fold cross-validation scheme. High classification rates were achieved. The DT algorithm outperformed the other emotion classification schemes in terms of higher emotion recognition rates. The highest classification accuracy of 100% was obtained for fear, neutral, and happy recognition, and the average accuracy was over 90%. The corresponding specificity and sensitivity were 100%. In contrast, the lowest emotion recognition rates were achieved using kNN.

Until now, Zheng *et al.* [18] explored the capacity of EEG and eye movements' characteristics in emotion recognition. They reported that eye movements outperformed EEG in classifying fear emotions. The results of our analysis are inconsistent with their results since it is impossible to assuredly say which excitement is more likely to be classified than another. Their best mean accuracy of the proposed algorithm was less than 70% using eye movement data, while our proposed scheme provided the best mean accuracy of 91.89%. Moreover, the performance of our algorithm has been much superior to that of the Lu *et al.* [17] algorithm. They reported the best average accuracy of 77.8% using eye movement analysis. Guo *et al.* [48] implemented a bimodal deep auto-encoder to classify the features obtained from EEG and eye movements. The proposed emotion classification scheme provides a maximum rate of 79.63%. Tarnowski *et al.* [27] evaluated different eye information, including pupil diameter, the fixations,

and saccades' eye movements. The highest accuracy was 80% for an SVM. Lamba and Virmani [49] proposed a multimodal system using an eye blink pattern and heart rate. The scheme aimed to categorize neutral, surprise, and happy faces, which obtained the highest accuracy rate of 78.40% using SVM. Paul *et al.* [50] analyzed EOG signals for recognizing positive, neutral, and negative emotions. They extracted Hjorth parameters and Discrete Wavelet Transforms (DWT) to characterize EOG. The scheme achieved the highest accuracy rate of 81% using the combination of SVM and DWT. Bao *et al.* [51] attempted to provide a gender-related emotion classification system. It was designated to recognize disgust, fear, sadness, neutral, and happy emotions while utilizing the EEG and eye-movement signals. Deep canonical correlation analysis and a bimodal-long short-term memory were introduced for classification. The highest mean accuracy rate was 46.89% using a deep canonical correlation model. Wang *et al.* [52] provided an emotive recognition system using EOG and eye movement video synchronously. Several time-domain eye movement features (fixation duration, saccade duration, and pupil diameter) and short-time Fourier transforms of multi-channel EOG signals were calculated. The feature-level and decision-level fusion strategies were tested to classify positive, neutral, and negative emotional states. The mean accuracies were 88.64 and 88.35% for the former and the latter fusion strategies, respectively. By integrating EEG and eye movement information, Su *et al.* [53] proposed a multimodal emotion intensity perception technique. Several temporal, spectral, and statistical features of the signals were extracted. The scheme resulted in the best recognition accuracies of 72.8 and 69.3% for the arousal and valence dimensions, respectively. Zheng *et al.* [54] introduced a multimodal emotion recognition framework. EEG feature map and eye-tracking measures were fed to the SVM. The best average accuracies were 71.77 and 58.90% for EEG signals and eye-tracking data, respectively. The accuracy rates increased to 73.59% and 72.98% using feature-level and decision-level fusion strategies, respectively. Liu *et al.* [55] attempted to provide a multimodal emotion recognition scheme using deep canonical correlation analysis. They assessed the approach on different databases. The results showed a maximum accuracy of 87.45% for two binary classification tasks on the SEED-IV database. In our recent experiment [56], we analyzed polar-based lagged Poincare plot measures of identical eye databases. The results highlighted an average

accuracy of 84.17% for fear and sad discrimination using SVM. Sarma and Barma [57] evaluated the blinking rate variability using different statistical, sample entropy, geometrical, and recurrence plot measures. They only evaluated the extracted features by reporting the mean values of the attributes in distinct emotional classes without doing any statistical test or classification.

The results of the present experiment were superior to all of these studies in terms of classification accuracy (Table 2). It should be noted that the same database (SEED-IV) that we applied in this article was just used in [18, 55, 56].

The results of this experiment are not comparable to other studies. In the previous research, neither the introduced processing approach, the visibility graph-

based indices, have been used to classify emotions, nor have the eye-blinking data in a single-modality form been analyzed for affect recognition. Additionally, limited studies used the same dataset that was used in the current study [18, 55, 56].

There are some limitations to be considered in the future. Our results verified a higher mean accuracy of 91.89% employing DT. An avenue for improving the performance is to implement other machine learning algorithms. In addition, we merged the data from all three sessions to classify emotion. However, whether recognition rates are affected by multiple trial days should be assessed. In the current study, we tested our methodology using an available database (SEED-IV) [18], which comprises the signals of 15 healthy

**Table 2.** Comparison of the achievements of some emotion classification schemes using eye data

Study	Single/Multi-modality	Methodology	Best average accuracy (%)
[51]	EEG and eye-movement signals	A deep canonical correlation analysis and a bimodal-long short-term memory	46.89
[26]	Single	Low-level and Statistical features, Gaussian Mixture Model	66
[53]	EEG and eye movement information	Temporal, spectral, and statistical features	72.8
[54]	EEG and eye tracking data	EEG feature map, eye tracking measures, SVM, feature-level and decision-level fusion	73.59
[49]	Eye blink pattern and heart rate	Pulse rate variability, eye blinking variability, Support vector machine	78.4
[48]	Multi: EEG and eye movements	Feature level fusion and Bimodal Deep Auto-Encoder	79.63
[27]	Single	Pupil diameter, the fixations and saccades' eye movements, SVM	80
[50]	Single: EOG	Hjorth parameters, DWT, SVM, and Naïve Bayes	81%
[18]	Multi: EEG and eye movements	PSD and differential entropy of EEG, 33 features of eye movements, deep neural networks	85.11
[55]	Multi: EEG and eye movements	deep canonical correlation analysis	87.45
[17]	Multi: EEG and eye movements	PSD and differential entropy of EEG, 33 features of eye movements, Fuzzy integral, Support vector machine	87.59
[52]	EOG and eye movement video	Time-domain eye movement features, short-time Fourier transforms of multi-channel EOG signals, feature-level and decision-level fusion	88.64
[56]	Single	Polar-based lagged Poincare plot measures, SVM	84.17
[57]	Single	Statistical, sample entropy, geometrical, and recurrence plot measures.	-
Current study	Single	Weighted Visibility Graph, kNN, SVM, AdaBoost, DT, RS	91.89

participants. Another drawback of the experiment is the limited number of data, which fails the experiments to verify the effectiveness of the proposed method. It is suggested to assess the framework using big data in the future. Bao *et al.* [51] showed the impact of a sex-specific factor on emotion recognition in which temporal blink features (duration and frequency) differed from male to female and negatively correlated under various affective states. Future works should investigate whether gender also affects the nonlinear characteristics of the signal and the classification rate. Other individual characteristics, such as age, should also be considered in the forthcoming study. A recent review article by Lim *et al.* [57] emphasized that the classification accuracy rate may be different between subject-dependent and subject-independent modes. Future work should evaluate the performance of the proposed system by considering this issue.

## 5. Conclusion

This research introduced a novel single-modality approach for emotion classification using eye-blinking data. The innovation of this work has laid in both the use of single-modality eye blinking signals and the feature extraction methodology. Visibility graph-based indices were extracted from the eye-blinking data for the first time. Then, the features were fed to the classifiers to complete the classification process. The suggested framework provided high performances, comparable with other previously reported results concerning high recognition rates. The highest mean recognition rate was > 90% for fear, neutral, and happy discrimination. The suggested framework can be extended for a future affect recognizer based on eye-blinking data.

## Acknowledgments

This research did not receive any specific grant from funding agencies in the public, commercial, or not-for-profit sectors”.

The authors declare that they have no conflict of interest.

In this article, SEED-IV database [18] has been evaluated, which is freely accessible at: <http://bcmi.sjtu.edu.cn/~seed/seed-iv.html>.

This article does not contain any studies with human participants performed by any of the authors.”

## References

- 1- Iris B. Mauss and Michael D. Robinson, "Measures of emotion: A review." *Cognition and Emotion*, Vol. 23 (No. 2), pp. 209-37, (2009).
- 2- Richard Sieb, "The Emergence of Emotions. Act Nerv Super, ()." *Activitas Nervosa Superior*, Vol. 55pp. 115–45, (2013).
- 3- Matteo Spezialetti, Giuseppe Placidi, and Silvia Rossi, "Emotion Recognition for Human-Robot Interaction: Recent Advances and Future Perspectives." *Frontiers in Robotics and AI*, Vol. 7p. 532279, (2020).
- 4- Moon Inder Singh and Mandeep Singh M, "Development of a real time emotion classifier based on evoked EEG." *Biocybernetics and biomedical engineering*, Vol. 37 (No. 3), pp. 498-509, (2017).
- 5- Matteo Spezialetti, Giuseppe Placidi, and Silvia Rossi, "Emotion Recognition for Human-Robot Interaction: Recent Advances and Future Perspectives." *Frontiers in Robotics and AI*, Vol. 7p. 532279, (2020).
- 6- Ateke Goshvarpour and Atefeh Goshvarpour, "A novel approach for EEG electrode selection in automated emotion recognition based on lagged Poincare's indices and sLORETA." *Cognitive Computation*, Vol. 12pp. 602–18, (2020).
- 7- Atefeh Goshvarpour and Ateke Goshvarpour, "EEG spectral powers and source localization in depressing, sad, and fun music videos focusing on gender differences." *Cognitive Neurodynamics*, Vol. 13pp. 161–73, (2019).
- 8- Mimma Nardelli, Gaetano Valenza, Alberto Greco, Antonio Lanata, and Enzo Pasquale Scilingo, "Recognizing Emotions Induced by Affective Sounds through Heart Rate Variability." *IEEE Transactions on Affective Computing*, Vol. 6 (No. 4), pp. 385–94, (2015).
- 9- Yu-Liang Hsu, Jeen-Shing Wang, Wei-Chun Chiang, and Chien-Han Hung, "Automatic ECG-Based Emotion Recognition in Music Listening." *IEEE Transactions on Affective Computing*, Vol. 11 (No. 1), pp. 85-99, (2020).
- 10- Ateke Goshvarpour, Ataollah Abbasi, and Atefeh Goshvarpour, "Do men and women have different ECG responses to sad pictures." *Biomedical Signal Processing and Control*, Vol. 38pp. 67-73, (2017).
- 11- Atefeh Goshvarpour, Ataollah Abbasi, and Ateke Goshvarpour, "An accurate emotion recognition system using ECG and GSR signals and matching pursuit method." *Biomedical Journal*, Vol. 40 (No. 6), pp. 355-68, (2017).
- 12- Atefeh Goshvarpour, Ataollah Abbasi, Ateke Goshvarpour, and Sabalan Daneshvar, "Discrimination

- between different emotional states based on the chaotic behavior of galvanic skin responses." *Signal, Image and Video Processing*, Vol. 11pp. 1347–55, (2017).
- 13- Atefeh Goshvarpour and Ateke Goshvarpour, "The potential of photoplethysmogram and galvanic skin response in emotion recognition using nonlinear features." *Physical and Engineering Sciences in Medicine*, Vol. 43pp. 119–34, (2020).
  - 14- Atefeh Goshvarpour and Ateke Goshvarpour, "Poincaré's section analysis for PPG-based automatic emotion recognition." *Chaos, Solitons & Fractals*, Vol. 114pp. 400-07, (2018).
  - 15- Atefeh Goshvarpour and Ateke Goshvarpour, "Evaluation of novel entropy-based complex wavelet sub-bands measures of PPG in an emotion recognition system." *Journal of Medical and Biological Engineering*, Vol. 40pp. 451–61, (2020).
  - 16- Anna Gruebler and Kenji Suzuki, "Design of a Wearable Device for Reading Positive Expressions from Facial EMG Signals." *IEEE Transactions on Affective Computing*, Vol. 5 (No. 3), pp. 227-37, (2014).
  - 17- Yifei Lu, Wei-Long Zheng, Binbin Li, and Bao-Liang Lu, "Combining eye movements and EEG to enhance emotion recognition." in *IJCAI'15: Proceedings of the 24th International Conference on Artificial Intelligence*, Buenos Aires, Argentina, (2015): AAAI Press, pp. 1170–76.
  - 18- Wei-Long Zheng, Wei Liu, Yifei Lu, Bao-Liang Lu, and Andrzej Cichocki, "Emotionmeter: A multimodal framework for recognizing human emotions." *IEEE Transactions on Cybernetics*, Vol. 49 (No. 3), pp. 1110-22, (2019).
  - 19- Jeffrey F Cohn, Jing Xiao, Tsuyoshi Moriyama, Zara Ambadar, and Takeo Kanade, "Automatic recognition of eye blinking in spontaneously occurring behavior." *Behavior research methods, instruments, & computers: a journal of the Psychonomic Society, Inc*, Vol. 35 (No. 3), pp. 420–28, (2003).
  - 20- Sarmad Al-gawwam, Mohammed Benaissa, and pp. 388-392 "Depression Detection from Eye Blink Features." in *2018 IEEE International Symposium on Signal Processing and Information Technology (ISSPIT)*, Louisville, KY, USA, (2018): IEEE.
  - 21- Judith Bek, Ellen Poliakoff, and Karen Lander, "Measuring emotion recognition by people with Parkinson's disease using eye-tracking with dynamic facial expressions." *Journal of neuroscience methods*, Vol. 331p. 108524, (2019).
  - 22- Behakti Sonawane and Priyanka Sharma, "Review of automated emotion-based quantification of facial expression in Parkinson's patients." *The Visual Computer*, Vol. 37pp. 1151–67, (2021).
  - 23- N.A. Martin-Key, E.W. Graf, W.J. Adams, and G. Fairchild, "Facial emotion recognition and eye movement behaviour in conduct disorder." *Journal of Child Psychology and Psychiatry*, Vol. 59 (No. 3), pp. 247-57, (2018).
  - 24- Melissa H Black *et al.*, "Mechanisms of facial emotion recognition in autism spectrum disorders: Insights from eye tracking and electroencephalography." *Neuroscience & Biobehavioral Reviews*, Vol. 80pp. 488-515, (2017).
  - 25- Allison Dornbach-Bender *et al.*, "Attention for emotion associated with hypomanic personality traits: Eye-tracking reveals a positive bias independent of mood." *Neurology, Psychiatry and Brain Research*, Vol. 32, June, Pages pp. 30-35, (2019).
  - 26- Sharifa Alghowinem, Majdah AlShehri, Roland Goecke, and Michael Wagner, "Exploring eye activity as an indication of emotional states using an eye-tracking sensor." in *Intelligent Systems for Science and Information. Studies in Computational Intelligence*, Vol. 542, Supriya Kapoor Liming Chen, Rahul Bhatia, Ed.: Springer, Cham, (2014), pp. 261–76.
  - 27- Paweł Tarnowski, Marcin Kołodziej, Andrzej Majkowski, and Remigiusz Jan Rak, "Eye-Tracking Analysis for Emotion Recognition." *Computational Intelligence and Neuroscience*, Vol. 2020p. 2909267, (2020).
  - 28- M. A. Savi, "Chaos and order in biomedical rhythms." *Journal of the Brazilian Society of Mechanical Sciences and Engineering*, Vol. 27 (No. 2), pp. 157-69, (2005).
  - 29- J. Zhang and M. Small, "Complex Network from Pseudoperiodic Time Series: Topology versus Dynamics." *Physical Review Letter*, Vol. 96 (No. 23), p. 238701, (2006).
  - 30- Lucas Lacasa, Bartolo Luque, Fernando Ballesteros, and Juan Carlos Nuño, "From time series to complex networks: The visibility graph." *Proceedings of the National Academy of Sciences*, Vol. 105 (No. 13), pp. 4972-75, (2008).
  - 31- B. Luque, L. Lacasa, F. Ballesteros, and J. Luque, "Horizontal visibility graphs: exact results for random time series." *Physical Review E*, Vol. 80 (No. 4), p. 046103, (2009).
  - 32- Anirban Bhaduri, Susmita Bhaduri, and Dipak Ghosh, "Visibility graph analysis of heart rate time series and biomarker of congestive heart failure." *Physica A: Statistical Mechanics and its Applications*; ,Vol. 482pp. 786-95, (2017).
  - 33- Marjan Mozaffarilegha and Hojjat Adeli, "Visibility graph analysis of speech evoked auditory brainstem response in persistent developmental stuttering." *Neuroscience Letters*, Vol. 696pp. 28-32, (2019).
  - 34- Supriya Supriya, Siuly Siuly, Hua Wang, Jinli Cao, and Yanchun Zhang, "Weighted Visibility Graph With Complex Network Features in the Detection of Epilepsy." *IEEE Access*, Vol. 4pp. 6554-66, (2016).

- 35- Rohit Bose, Kaniska Samanta, Sudip Modak, and Soumya Chatterjee, "Augmenting Neuromuscular Disease Detection Using Optimally Parameterized Weighted Visibility Graph." *IEEE Journal of Biomedical and Health Informatics*, Vol. 25 (No. 3), pp. 685-92, (2021).
- 36- Mohammed Diykh, Yan Li, and Shahab Abdulla, "EEG sleep stages identification based on weighted undirected complex networks." *Computer Methods and Programs in Biomedicine*, Vol. 184p. 105116, (2020).
- 37- Guohun Zhu, Yan Li, and Peng Wen, "Analysis and Classification of Sleep Stages Based on Difference Visibility Graphs From a Single-Channel EEG Signal, *IEEE J Biomed Health Inform*; 18(6): . doi:." *IEEE Journal of Biomedical and Health Informatics*, Vol. 18 (No. 6), pp. 1813-21, (2014).
- 38- Ruofan Wang, Zhongyou Yang, Jiang Wang, and Lianshuan Shi, "An Improved Visibility Graph Analysis of EEG Signals of Alzheimer Brain." Presented at the *11th International Congress on Image and Signal Processing, BioMedical Engineering and Informatics (CISP-BMEI)*, Beijing, China, (2018).
- 39- Gulraiz Iqbal Choudhary, Wajid Aziz, Ishtiaq Rasool Khan, Susanto Rahardja, and Pasi Fränti, "Analysing the Dynamics of Interbeat Interval Time Series Using Grouped Horizontal Visibility Graph." *IEEE Access* Vol. 7pp. 9926-34, (2019).
- 40- Susmita Bhaduri, Agniswar Chakraborty, and Dipak Ghosh, "Speech emotion quantification with chaos-based modified visibility graph-possible precursor of suicidal tendency." *Journal of Neurology and Neuroscience*, Vol. 7 (No. 3), p. 100, (2016).
- 41- Kaniska Samanta, Soumya Chatterjee, and Rohit Bose, "Cross-Subject Motor Imagery Tasks EEG Signal Classification Employing Multiplex Weighted Visibility Graph and Deep Feature Extraction, *IEEE Sens. Lett.* 2020; 4(1): . doi: ." *IEEE Sensors Letters*, Vol. 4 (No. 1), p. 7000104, (2020).
- 42- Antonio Maffei and Alessandro Angrilli, "Spontaneous blink rate as an index of attention and emotion during film clips viewing." *Physiology & Behavior*, Vol. 204 (No. 15), pp. 256-63, (2019).
- 43- S. Iglin. (2020). grTheory - Graph Theory Toolbox (<https://www.mathworks.com/matlabcentral/fileexchange/4266-grtheory-graph-theory-toolbox>). Retrieved July 6, 2020, *MATLAB Central File Exchange*. [Online]. Available.
- 44- R.W. Floyd, "Algorithm 97: shortest path." *Communications of the ACM*, Vol. 5 (No. 6), p. 345, (1962).
- 45- Raof Gholami and Nikoo Fakhari, "Chapter 27 - Support Vector Machine: Principles, Parameters, and Applications." in *Handbook of Neural Computation*. , Pages . Pijush Samui, Sanjiban Sekhar, and Valentina E. Balas, Eds.: *Academic Press*, (2017), pp. 515-35.
- 46- Micheline Kamber Jiawei Han, Jian Pei, Data mining: Concepts and techniques. 3 ed. *Elsevier*, (2011), p. 744.
- 47- Daniel T. Larose, Discovering knowledge in data: An introduction to data mining. *John Wiley & Sons*, (2014).
- 48- Wei Liu, Jie-Lin Qiu, Wei-Long Zheng, and Bao-Liang Lu, "Multimodal Emotion Recognition Using Deep Canonical Correlation Analysis. :1908.05349v1 [cs.LG] 13 Aug " *Machine Learning (cs.LG); Computer Vision and Pattern Recognition (cs.CV)*. DOI: <https://arxiv.org/abs/1908.05349>
- 49- Puneet Singh Lamba and Deepali Virmani, "Information Retrieval from Emotions and Eye Blinks with help of Sensor Nodes." *International Journal of Electrical and Computer Engineering (IJECE)*, Vol. 8 (No. 4), pp. 2433-41, (2018).
- 50- Sananda Paul, Anwesha Banerjee, and D.N. Tibarewala, "Emotional eye movement analysis using electrooculography signal." *International Journal of Biomedical Engineering and Technology*, Vol. 23 (No. 1), pp. 59–70, (2017).
- 51- Lan-Qing Bao, Jie-Lin Qiu, Hao Tang, Wei-Long Zheng, and Bao-Liang Lu, "Investigating Sex Differences in Classification of Five Emotions from EEG and Eye Movement Signals." Presented at the *Annual International Conference of the IEEE Engineering in Medicine and Biology Society. IEEE Engineering in Medicine and Biology Society*, (2019).
- 52- Yang Wang, Zhao Lv, and Yongjun Zheng, "Automatic Emotion Perception Using Eye Movement Information for E-Healthcare Systems." *Sensors (Basel)*, Vol. 18 (No. 9), p. 2826, (2018).
- 53- Yuanyuan Su, Wenchao Li, Ning Bi, and Zhao Lv, "Adolescents Environmental Emotion Perception by Integrating EEG and Eye Movements." *Frontiers in neurorobotics*, Vol. 13p. 46, (2019).
- 54- Wei-Long Zheng, Bo-Nan Dong, and Bao-Liang Lu, "Multimodal emotion recognition using EEG and eye tracking data." *Annual International Conference of the IEEE Engineering in Medicine and Biology Society. IEEE Engineering in Medicine and Biology Society*, Vol. 2014pp. 5040-43, (2014).
- 55- Wei Liu, Jie-Lin Qiu, Wei-Long Zheng, and Bao-Liang Lu, "Multimodal Emotion Recognition Using Deep Canonical Correlation Analysis. :1908.05349v1 [cs.LG] 13 Aug " *Machine Learning (cs.LG); Computer Vision and Pattern Recognition (cs.CV)*. DOI: <https://arxiv.org/abs/1908.05349>
- 56- Atefeh Goshvarpour and Ateke Goshvarpour, "Human emotion recognition using polar-based lagged Poincare plot indices of eye-blinking data." *International Journal of Computational Intelligence and Applications*, Vol. 20 (No. 4), p. 2150023 (15 pages), (2021).
- 57- Parthana Sarma and Shovan Barma, "Usefulness of blinking duration variability (BDV) in discriminating emotional states." *Biomedical Signal Processing and Control*, Vol. 69p. 102883, (2021).